sustainability

Article

Selection of Optimum Working Fluid for Organic Rankine Cycles by Exergy and Exergy-Economic Analyses

Kamyar Darvish [1], Mehdi A. Ehyaei [2,*], Farideh Atabi [1] and Marc A. Rosen [3]

[1] Department of Environmental and Energy Engineering, Science and Research Branch, Islamic Azad University, Tehran 13967-33364, Iran; E-Mails: k.darvish@goldiranac.com (K.D.); far-atabi@jamejam.net (F.A.)

[2] Department of Mechanical Engineering, Pardis Branch, Islamic Azad University, Pardis New City 14778-93855, Iran

[3] Faculty of Engineering and Applied Science, University of Ontario Institute of Technology, 2000 Simcoe Street North, Oshawa, ON L1H 7K4, Canada; E-Mail: marc.rosen@uoit.ca

* Author to whom correspondence should be addressed; E-Mail: aliehyaei@yahoo.com; Tel.: +98-9123478028.

Abstract: The thermodynamic performance of a regenerative organic Rankine cycle that utilizes low temperature heat sources to facilitate the selection of proper organic working fluids is simulated. Thermodynamic models are used to investigate thermodynamic parameters such as output power, and energy efficiency of the ORC (Organic Rankine Cycle). In addition, the cost rate of electricity is examined with exergo-economic analysis. Nine working fluids are considered as part of the investigation to assess which yields the highest output power and exergy efficiency, within system constraints. Exergy efficiency and cost rate of electricity are used as objective functions for system optimization, and each fluid is assessed in terms of the optimal operating condition. The degree of superheat and the pressure ratio are independent variables in the optimization. R134a and iso-butane are found to exhibit the highest energy and exergy efficiencies, while they have output powers in between the systems using other working fluids. For a source temperature was equal to 120 °C, the exergy efficiencies for the systems using R134a and iso-butane are observed to be 19.6% and 20.3%, respectively. The largest exergy destructions occur in the boiler and the expander. The electricity cost rates for the system vary from 0.08 USD/kWh to 0.12 USD/kWh, depending on the fuel input cost, for the system using R134a as a working fluid.

1. Introduction

Nowadays, renewable energy resources such as solar, geothermal and wind, as well as heat losses from a wide range of industries, are increasingly being considered as energy sources that can help meet the world's demand. Waste heat is often at relatively low temperatures, making it very difficult to convert such heat to electrical energy via conventional methods. As a result, many potential heat sources are wasted. Research on how to convert such heat resources to electricity is ongoing. Various cycles such as the organic Rankine, supercritical Rankine, Kalina, Goswami, and trilateral flash cycles have been investigated for electrical power production from low temperature heat resources [1].

The operating principles for organic and steam-based Rankine cycles are similar. The main difference is the choice of working fluid. Refrigerants such as butane, pentane, hexane and silicon oil, which have lower boiling temperatures than water, can be used as working fluids in organic Rankine cycles (ORCs). These fluids are heated with low temperature heat like recovered waste heat and have properties that differ from those of water in many respects.

Organic Rankine cycles have been studied both theoretically [2,3] and experimentally [4] since the 1970s, and exhibit efficiencies lower than 10% for small-scale systems. The first commercial organic Rankine cycles, which used geothermal and solar heat sources, appeared between 1970 and 1980. Numerous organic Rankine cycles have been installed in some countries (e.g., USA, Canada, Italy and Germany), although applications have also been reported in Finland, Belgium, Swaziland, Austria, Russia, Romania, India and Morocco.

There are numerous ORC equipment suppliers. Ormat and Turboden produce units for waste heat recovery for various industries (oil and gas, biomass, energy, packaging, cement and glass). The Swedish companies Upon AB and Entrans have installed several Organic Rankine cycles in Sweden in recent years. Upon AB has developed the Upon Power Box, a technology to generate electrical power from waste heat. Organic Rankine cycles with a total capacity of more than 1800 MWe are installed today around the world, most linked to biomass combined heat and power (CHP) and geothermal heat sources [5].

The basic configuration and thermodynamic principles of steam and organic Rankine cycles are similar, but working fluids with thermodynamic properties that best suit the heat source are selected for organic Rankine cycles. Organic Rankine cycles have numerous advantages over conventional electrical generation systems:

- Lower temperature applications
- Low operation and maintenance costs
- Compactness
- No water consumption in some models
- Smaller expanders with higher rotational speeds
- Quiet operation
- Simple start/stop procedures

Another advantage of organic working fluids is that the turbine in ORC requires a single-stage expander. This makes organic Rankine cycles simpler and more economic than typical Rankine cycles [6]. Applications of ORCs include the following:

- Biomass
- Geothermal energy
- Solar
- Heat recovery

The saturation curve slope for organic working fluids can be positive (iso-pentane), negative (R22) or vertical (R11). These fluids are called "wet", "dry" and "isentropic" fluids, respectively. Wet fluids (water) usually need to be superheated for electrical generation applications. Other organic fluids, of the dry or isentropic types, do not need to be superheated.

Much research has been carried out on organic Rankine cycles and their working fluids. Hung *et al.* investigated efficiencies of ORCs using benzene, ammonia, R11, R12, R134a and R113 as working fluids. They concluded that isentropic fluids were the most suitable for recovering low-temperature waste heat [7]. Angelino and Colonna developed a computer code with a commercial package for ORC analysis and optimization [8]. Yamamoto *et al.* investigated an ORC using HCFC-123 as a working fluid and conclude that this system has a better efficiency than one using water as a working fluid [9]. Nguyen *et al.* designed a Rankine cycle using n-pentane as the working fluid. This system produces 1.5 kW of electricity with a thermal efficiency of 4.3% [10].

Wei *et al.* reported a performance assessment and optimization of an ORC using HFC-245fa (3-pentafluoropropane) as a working fluid. The cycle was driven by exhaust heat. They concluded that usage of exhaust heat is a good way to improve system net power output and efficiency [11]. Saleh *et al.* investigated 31 pure components as working fluids for organic Rankine cycles. They concluded that ORCs typically operate between 100 and 30 °C for geothermal power plants at pressures mostly limited to 20 bar, but in some cases supercritical pressures are also considered. Thermal efficiencies are presented for various cycles. In the case of subcritical pressure processes, one has to identify (1) whether the shape of the saturated vapor line in the T-s diagram is bell-shaped or overhanging; and (2) whether the vapor entering the turbine is saturated or superheated. Moreover, for the case where the vapor leaving the turbine is superheated, an internal heat exchanger (IHE) may be used. The highest thermal efficiencies are obtained for high-temperature boiling substances with an overhanging saturated vapor line in subcritical processes within an IHE, e.g., for n-butane the thermal efficiency is 0.130. On the other hand, a pinch analysis of the heat transfer for the heat carrier with a maximum temperature of 120 °C to the working fluid shows that the largest amount of heat can be transferred to a supercritical fluid and the least to a high boiling temperature subcritical fluid [12].

Mago and Chamra performed an exergy analysis of a combined engine-organic Rankine cycle, and conclude that the ORC with an engine improves the first and second law efficiencies [13]. Mago *et al.* analyzed regenerative organic Rankine cycles using dry organic working fluids; the cycles convert waste heat to electricity. The dry organic fluids considered are R113, R245ca, R123, and isobutane, which have boiling points ranging from −12 °C to 48 °C. The regenerative ORC was analyzed and compared with a basic ORC in order to determine the configuration that presents the best thermal efficiency and minimum irreversibility. The authors demonstrated that a regenerative ORC has a higher efficiency

than the basic ORC, and also releases less waste heat when producing the same electricity with less irreversibility [14].

Chacartegui *et al.* investigated low temperature organic Rankine cycles as bottoming cycles in medium and large scale combined cycle power plants. The following organic working fluids were considered: R113, R245, isobutene, toluene, cyclohexane and isopentane. Competitive results were obtained for ORC combined cycles using toluene and cyclohexane as working fluids; as such, the systems exhibited reasonably high global efficiencies [15].

Dai *et al.* investigated ORCs for low-grade waste heat recovery with different working fluids. Thermodynamic properties for each working fluid were investigated and the cycles were optimized with exergy efficiency as an objective function using genetic algorithms. The authors showed that the cycles with organic working fluids were better than the cycle with water for converting low-grade waste heat to useful work. The cycle with R236EA exhibits the highest exergy efficiency. Adding an internal heat exchanger to the ORC did not improve the performance under the given waste heat conditions [16].

Quoilin *et al.* performed thermodynamic and economic optimizations of small-scale ORCs for waste-heat recovery applications, considering R245fa, R123, n-butane, n-pentane and R1234yf and Solkatherm as working fluids. They determined that the operating point for maximum power did not correspond to that of the minimum specific investment cost [17].

Wang *et al.* analyzed the performance of nine pure organic fluids at specific operating regions and foud that R11, R141b, R113 and R123 exhibited slightly better thermodynamic performances than the others, and that R245fa and R245ca were the most environmentally benign working fluids for engine waste heat-recovery applications [18].

Qiu compared and optimized the eight most commonly applied working fluids and developed a performance ranking by means of the spinal point method [19].

Hun Kang theoretically and experimentally investigated an ORC for generating electric power using a low-temperature heat source, using R245fa as a working fluid [20].

Wang *et al.* modeled a regenerative organic Rankine cycle for utilizing solar energy over a range of low temperatures, considering flat-plate solar collectors and thermal storage systems. They showed that system performance could be improved, under realistic constraints, by increasing turbine inlet pressure and temperature or lowering the turbine backpressure, and by using a higher turbine inlet temperature with a saturated vapor input. Compared to other working fluids, R245fa and R123 were identified as the most suitable for the system, in part due to their low operation pressures and the good performance they fostered [21]. Quoilin *et al.* described ORC applications, markets and costs, working fluid selection, and expansion machine issues [22].

Clement *et al.* presented an ORC system for recovering heat from a 100 kWe commercial gas turbine with an internal recuperator. They optimized the thermodynamic cycles, considering six working fluids, and analyzed several expanders to determine the most suitable [23]. Branchini *et al.* evaluated six thermodynamic indexes: cycle efficiency, specific work, recovery efficiency, turbine volumetric expansion ratio, ORC fluid-to-hot source mass flow ratio and heat exchanger size, for several cycle configurations: recuperation, superheated, supercritical, regenerative and combinations [24]. Lecomptea *et al.* developed a thermoeconomic design methodology for an ORC based on specific investment cost, operating conditions and part load behavior, which permitted selection of the optimum cycle [25].

Zabek *et al.* optimized a heat-to-power conversion process by maximizing the net power output. The process employed a trans-critical ORC with R134a as the working fluid. The authors developed a positive heat exchange/pressure correlation for the net power output with reasonable cycle efficiencies of around 10% for moderate device sizes, and concluded that, in order to design a comprehensive and dynamic unit configuration, a flexible cycle layout with an adjustable working fluid mass flow is required [26]. Bracco *et al.* experimentally tested and numerically modeled under transient conditions a small ORC, for which the main components are the R245fa working fluid, a plate condenser, an inverter-driven diaphragm pump, an electric boiler and a scroll expander. The latter is a hermetic device, derived from a commercial HVAC compressor, which generates about 1.5 kW of electrical power. Performance parameters for the overall cycle and its components were investigated and it was found that the lab management system software was able to simulate systems in transient conditions [27]. Wang *et al.* proposed an ideal ORC model to analyze the influence of working fluid properties on the thermal efficiency. The optimal operation conditions and the exergy destructions for various heat resource temperatures were also evaluated utilizing pinch and exergy analyses. The authors demonstrated that the Jacob number and the ratio of evaporating temperature and condensing temperature have significant influences on the thermal efficiency of an ORC and that a low Jacob number indicates attractive performance for a given operation condition [28]. Yu *et al.* simulated an actual organic Rankine cycle bottoming system using R245fa as a working fluid for a diesel engine, and conclude that approximately 75% and 9.5% of the waste heat from exhaust gas and from jacket water, respectively, can be recovered [29]. Li *et al.* experimentally analyzed the effect of varying working fluid mass flow rate and regenerator on the efficiency of a regenerative ORC operating on R123, and find that the power output is 6 kW and the regenerative ORC efficiency is 8.0%, which is 1.8% higher than that of the basic ORC [30]. Maizza *et al.* thermodynamically optimized ORCs for power generation and CHP considering various average heat source profiles (waste heat recovery, thermal oil for cogeneration and geothermal) They develop optimization methods for subcritical and trans-critical, regenerative and non-regenerative cycles, and present an optimization model to predict the best cycle performance (subcritical or trans-critical) in terms of exergy efficiency, considering various working fluids [31]. Meinel *et al.* presented Aspen Plus (V7.3) simulations of a two-stage organic Rankine cycle with internal heat recovery for four working fluids, in a two-part study. First, the exhaust gas outlet was constrained to 130 °C to stay above the acid dew point; Second, the pinch point of the exhaust gas heat exchanger was set to 10 K. For wet and isentropic fluids, the thermodynamic efficiencies of the two-stage cycle exceeded the corresponding values of reference processes by up to 2.2%, while the recuperator design benefited from using dry fluids compared to the two-stage concept [32].

Mango *et al.* presented a second-law analysis for the use of organic Rankine cycle (ORC) to convert waste energy to power from low-grade heat sources. The working fluids under investigation are R134a, R113, R245ca, R245fa, R123, isobutene, and propane, with boiling points between 243 and 48 °C. Some of the results demonstrated that ORC using R113 showed the maximum efficiency among the evaluated organic fluids for temperatures <380 K, and isobutene showed the best efficiency [33].

Bu *et al.* investigated system efficiency on six working fluids, R123, R134a, R245fa, R600a (isobutene), R600 (butane) and R290, in order to using geothermal energy as a heat source. The calculated results show that R290 and R134a, R600a (isobutene) is the more suitable working fluid for ORC in terms of expander size parameter, system efficiency and system pressure [34].

In the present study, the thermodynamic performance of regenerative organic Rankine cycles utilizing low temperature heat sources is simulated to assist in selecting proper organic working fluids. Bristol and thermodynamic models are used to investigate thermodynamic parameters such as output power and efficiency, and the cost rate of the product electricity is determined with exergo-economic analysis. Nine working fluids are considered in order to investigate which yields the greatest output power and exergy efficiency within system constraints. Exergy efficiency and cost rate of electricity are used as objective functions for the system optimization. Each of fluid is examined in order to achieve optimal operating conditions. The degree of superheat and pressure ratio are independent variables in the optimization.

2. System Modeling

2.1. System Description

Figure 1 shows the regenerative organic Rankine cycle considered in the analysis. It is comprised of a boiler, expander, regenerator, condenser and pump. In the regenerator heat exchanger, heat is transferred between the high temperature vapor at the expander outlet and the low temperature fluid at the pump outlet in order to avoid energy loss. The reason for this is that, when using an isentropic or dry fluid, the expander exit flow is superheated. Depending on the working fluid and the expander pressure ratio, this temperature is higher than that of the flow exiting the pump. After the working fluid leaves the regenerator, it enters the boiler and absorbs heat from the heat source. The working-fluid phase varies from a sub-cooled liquid to a saturated or superheated vapor. Then the saturated or superheated vapor passes through the expander linked to an electric generator, which converts the energy of vapor to electrical energy. The working fluid exiting the regenerator enters the condenser where heat is rejected to environment. The working fluid condenses and heat is rejected to a heat sink.
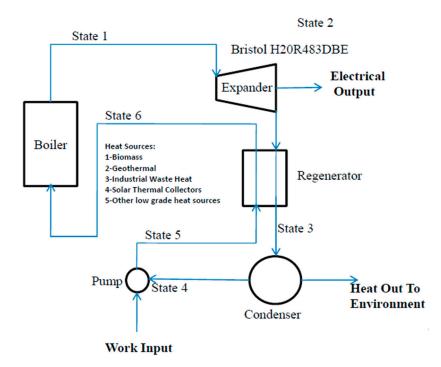

Figure 1. Diagram of regenerative organic Rankine cycle.

The following assumptions are invoked to simplify the analysis:

- The generator efficiency is constant at 85%.
- The expander inlet temperature is constant at 110 °C.
- The pump isentropic efficiency is constant at 85%.
- The environment temperature and pressure are taken to be 25 °C and 101.325 kPa, respectively.
- Heat losses from the turbine, piping and pump are negligible.
- The regenerator has an effectiveness of 0.8.
- Temperature difference between states 3 and 4 is 5 °C.
- The heat source temperature is 120 °C. Since the system is designed for many types of low temperature heat sources such as solar or industrial heat so the heat source temperature in this study is considered 120 °C.
- The system is at steady state.

2.2. Working Fluid Selection

Working fluid selection is one of the most important considerations in ORC design. For working fluid selection, several criteria need to be considered: environmental sustainability, ozone depletion potential, (ODP) global warming potential (GWP), safety (non-flammable, non-toxic and non-corrosive), vapor pressure in boiler, critical temperature, and thermal stability. Nine working fluids are selected for analysis of the behavior of the ORC cycle. Table 1 shows the basic properties for the selected working fluids.

Table 1. Basic properties of working fluids.

Fluid	Critical Temperature (°C)	Critical Pressure (kPa)	Density * (kg/m^3)	Heat of Vaporization ** (kJ/kg)
R134a	101	4059	4.258	217
R227ea	102.8	2999	7.148	131.7
R245fa	154	3651	5.718	196
R123	183.68	3668	1464	170.6
R600	151.98	3796	2.441	358
Toluene	318.6	4126	862.2	361.3
Iso-butane	134.7	3640	2.44	165.5
Iso-pentane	187.2	3370	614.5	342.5
n-pentane	196.5	3364	620.8	358

* Density at Room Temperature (25 °C) 1 atm; ****** Heat of Vaporization at 1 atm.

2.3. Thermodynamic Analysis

The expander used in the system considered is based on model H20R483DBE by Bristol. Oralli and Tarique investigate using a refrigeration scroll compressor as an expander for power generation applications using a Rankine cycle [35,36]. They develop a model applicable to using a scroll expander for determining the expansion process details, dissipation and leakage losses [36]. Figure 2 is the system diagram of the model proposed by Tarique [36]. The model considers isentropic expansion, which is limited by the built in volumetric ratio. The next step is a constant volume pressure rise, as calculated

with a constant specific to the expander. The constant is used to calculate the enthalpy of the fluid at the exit of this process, and takes into account internal frictional losses and other irreversibilities, which cause non-isentropic operation. The last step is to undergo a constant volume pressure rise or a constant enthalpy pressure drop, depending on the pressure ratio and the fluid. Finally the fluid mixes with the fluid, which has leaked internally to form state 2.
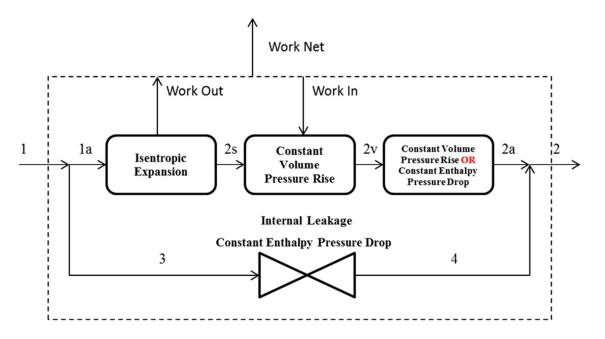

Figure 2. Scroll expander thermodynamic model diagram.

The leakage mass flow rate is calculated as follows [35]:

$$\dot{m}_{leak} = \zeta \sqrt{\frac{P_1}{v_1} - \frac{P_4}{v_4}} \tag{1}$$

Based on leakage flow rate, the mass flow rate exiting the expander is determined [35]:

$$\frac{\dot{m}_{exp}}{\dot{m}_{leak}} = 2 \times \left(\frac{h_1 - h_{2s}}{h_{2a} - h_{2s}} \right) \tag{2}$$

The coefficient used to calculate the exit conditions at the constant volume pressure building section is called the "isochoric pressure building coefficient" (Π). This is used to determine state 2v in Figure 2. The isochoric pressure building coefficient is defined as follows [36]:

$$\Pi = \frac{h_{2v} - h_{2s}}{h_1 - h_{2s}} \tag{3}$$

The next part of the model relates pressure forces with angular velocity and torque. The toque–pressure drop coefficient follows [36]:

$$\tau_{pf} = k_p \times \Delta p \tag{4}$$

$$\tau_{acc} = k_\omega \omega^2 m_{pocket} \tag{5}$$

$$\tau_{out} = \tau_{pf} - \tau_{acc} \tag{6}$$

$$\omega = 2\pi \times RPS \tag{7}$$

The coefficients used in the analysis for the Bristol H20R483DBE are shown in Table 2 [36].

Table 2. Parameters for the thermodynamic model of the Bristol expander.

Parameter	Value
BVR	2.9
Π	0.38
ζ	5.67×10^{-7}
k_ω	0.01733
k_p	4.960×10^{-6}

Once a suitable model is applied for the expander, a thermodynamic model for the system is needed to evaluate the system performance with the selected expander. For each component in the system, mass, enthalpy, entropy, and exergy balance equations are written for steady state operation, and these are shown below. The system is designed for many types of low temperature heat sources such as solar thermal energy and industrial waste heat. In this system, the boiler output temperature (state 1) is assumed to be constant at 110 °C, while the source temperature is assumed to be at 120 °C.

An energy balance for the boiler is:

$$q_{inb} = h_1 - h_6 \tag{8}$$

An exergy rate balance for the boiler is:

$$\dot{E}x_6 + \dot{E}x_{in} = \dot{E}x_1 + \dot{E}x_{db} \tag{9}$$

where $\dot{E}x_{in}$ is:

$$\dot{E}x_{in} = \left[1 - \left(\frac{T_0 + 273}{T_s + 273}\right)\right] \times \dot{Q}_{inb} \tag{10}$$

The turbine isentropic efficiency is defined as:

$$\eta_s = \frac{h_1 - h_2}{h_1 - h_{2s}} \tag{11}$$

The power output for the turbine can be expressed as:

$$\dot{W}_{out} = \dot{m}_{exp} \times (h_1 - h_{2a}) \tag{12}$$

The work rate output is also calculated as follows:

$$\dot{W}_{out} = \tau_{out} \times \omega \tag{13}$$

An exergy rate balance for the expander can be written as:

$$\dot{E}x_1 = \dot{E}x_2 + \dot{W}_{out} + \dot{E}x_{dexp} \tag{14}$$

The specific work lost to due to friction and other losses can be expressed as:

$$w_{loss} = h_{2ae} - h_{2se} \tag{15}$$

where the subscript e represents the expander. The regenerator is assumed to have an effectiveness of 0.8, implying that the actual amount of heat transferred is 80% of the possible energy transfer from states 2 to 3. The regenerator effectiveness is defined as:

$$\varepsilon_{regen} = \frac{q_{regen,out}}{q_{regen,in}} \tag{16}$$

where

$$q_{regen,out} = h_6 - h_5 \tag{17}$$

$$q_{regen.in} = h_2 - h_3 \tag{18}$$

State 3 is assumed to be at a temperature 5 °C higher than the condenser saturation temperature. Using an effectiveness (ε_{regen}) of 0.8, state 6 is calculated with the equation above. An exergy rate balance for the regenerator can be written as:

$$\dot{E}x_2 + \dot{E}x_5 = \dot{E}x_3 + \dot{E}x_6 + \dot{E}x_{dregen} \tag{19}$$

The condenser specific energy balance follows:

$$q_{out} = h_3 - h_4 \tag{20}$$

The exergy rate balance for the condenser:

$$\dot{E}x_3 = \dot{E}x_4 + \dot{E}x_{qout} + \dot{E}x_{qout1} + \dot{E}x_{dcond} \tag{21}$$

where

$$\dot{E}x_{qout} = \left[1 - \left(\frac{T_0 + 273}{T_4 + 273}\right)\right] \times (\dot{Q}_{out} - \dot{Q}_{outsv}) \tag{22}$$

$$\dot{E}x_{qout1} = \left[1 - \left(\frac{T_0 + 273}{T_{condavg} + 273}\right)\right] \dot{Q}_{outsv} \tag{23}$$

$$T_{cond,avg} = \frac{(T_3 + T_4)}{2} \tag{24}$$

$$\dot{Q}_{out,sv} = \dot{m}(h_3 - h_{3sv}) \tag{25}$$

$$\dot{Q}_{out} = \dot{m}q_{out} \tag{26}$$

The pump isentropic efficiency is taken to be 0.7, and the specific enthalpy at state 5 is calculated using:

$$h_5 = \left[(h_{5s} - h_4) \times \left(\frac{1}{\eta_{pump}}\right)\right] + h_4 \tag{27}$$

where h_{5s} is the ideal exit specific enthalpy if the pump is isentropic.

The exergy rate balance for the pump can be written as:

$$\dot{E}x_4 + \dot{W}_{in} = \dot{E}x_5 + \dot{E}x_{dpump} \tag{28}$$

where

$$\dot{W}_{in} = \dot{m}(h_5 - h_4) \tag{29}$$

The system efficiencies include energy and exergy efficiencies, with exergy efficiency being the objective function for optimization. The energy efficiency of the generator is set at 0.8. The energy (η_{th}) and exergy (η_{ex}) efficiencies for the system can be expressed as:

$$\eta_{th} = \frac{\dot{W}_{elec}}{\dot{Q}_{in}} \tag{30}$$

$$\eta_{ex} = \frac{\dot{W}_{elec}}{\dot{E}_{x_{in}}} \tag{31}$$

where

$$\dot{W}_{net} = \dot{W}_{out} - \dot{W}_{pump} \tag{32}$$

2.4. Exergo-Economic Analysis

Exergo-economic analysis determines the specific costs on the exergy streams in the exergy balance equations for each component of the system, as well as the capital and operating costs, in order to obtain a complete cost analysis. A typical cost rate balance for a component is given below:

$$\sum \dot{C}_{in} + \dot{W} \times c_{ein} + \dot{Z} = \sum \dot{C}_{out} + \dot{W} \times c_{eout} \tag{33}$$

where

$$\dot{C} = c \times \dot{E}x \tag{34}$$

The capital and operating costs for the components are expressed here in units of USD/h (US dollars per hour). For the system considered, a costing analysis is done to estimate the initial capital cost (ICC) and the operating and maintenance costs (OM). An amortization factor is used to amortize the cost of the sum of ICC and OM over 20 years at a 5% interest rate, and is determined as follows [37]:

$$A_f = \frac{i(i+1)^n}{(1+i)^n - 1} \tag{35}$$

Total costs for each of the components in the system are assessed in USD/h in the cost rate balance equations. After the initial capital and operating and maintenance costs are added and amortized, the total costs are divided by the number of hours in a year to obtain a cost in USD/h. Operating and maintenance costs are assumed to be a percentage of the initial capital costs. The general equations are given in below:

$$TCC_x = A_f(ICC_x + OM_x) \tag{36}$$

$$OM_x = ICC_x \times OM\% \tag{37}$$

$$\dot{Z}_x = \frac{TCC_x}{t_x} \tag{38}$$

The percentages for operating and maintenance costs are taken from Nafey *et al.* [36], while the costs for components are from various vendors. The cost rate balances for each of the components are developed to complete the exergo-economic analysis. The cost of the pump and condenser are added to the total capital and operating cost rate for the expander since the exergy stream in these components

have negligible values. The cost rate for the exergy leaving the expander is assumed to be 50% of the value entering, as this is lower temperature heat that is of less use. Exergy cost rates for the inlet and outlet of the condenser and pump are zero since these streams have little useable energy. Cost rate balances for each of the components (boiler, expander and regenerator) are shown below.

The exergy cost rate for the flow at state 1 and the boiler exergy cost rate balance, respectively, are as follows:

$$\dot{Ex}_1 = \dot{m} \times ex_1 \tag{39}$$

$$\left(\dot{Ex}_{in} \times c_f\right) + \left(\dot{Ex}_6 \times c_6\right) + \dot{Z}_b = \dot{Ex}_1 \times c_1 \tag{40}$$

The expander exergy cost rate balance, the state 2 exergy cost rate, and the electricity cost rate can be written as follows:

$$c_2 = c_1 \times 0.5 \tag{41}$$

$$\dot{Ex}_2 = \dot{m} \times ex_2 \tag{42}$$

$$\left(\dot{Ex}_1 \times c_1\right) + \dot{Z}_{exp} = \left(\dot{W}_{elec} \times c_e\right) + \left(c_2 \times \dot{Ex}_2\right) \tag{43}$$

$$\dot{C}_e = c_e \times \dot{W}_{elec} \tag{44}$$

The regenerator exergy cost rate balance and the state 6 exergy cost rate follow:

$$\dot{Ex}_6 = ex_6 \times \dot{m} \tag{45}$$

$$c_2 \times \dot{Ex}_2 + \dot{Z}_{regen} = \dot{Ex}_6 \times c_6 \tag{46}$$

Table 3 lists the costs for each of the components and the equations used to determine the final capital and operating rate $(\dot{Z}_x)$.

Table 3. Costing values and equations for the various parts of the system.

Component	ICC (USD)	OM% (% of ICC)	OM (USD)	TCC (USD/y)	$\dot{Z}_x$ (USD/h)
Boiler	600	15	90	55.37	0.0063
Expander	1000	25	250	100.3	0.0114
Regenerator	400	15	60	36.92	0.0042
Condenser	600	15	90	55.37	0.0063
Pump	300	25	75	30.1	0.0034

3. Optimization Modeling

Objective Function

The objective function for the thermodynamic optimization is the system exergy efficiency:

$$\eta_{Ex} = \frac{\dot{W}_{elec}}{\dot{Ex}_{in}} \tag{47}$$

where

$$\dot{Ex}_{in} = \left[1 - \left(\frac{T_0 + 273}{T_s + 273}\right)\right] \times \dot{Q}_{inb} \tag{48}$$

The objective function for the exergo-economic analysis is electricity cost rate, which is to be minimized here. The cost rate of electricity can be written as follows:

$$c_e = \frac{\dot{Ex}_1 \times C_1 + \dot{Z}_{exp} - c_2 \times \dot{Ex}_2}{\dot{W}_{elec}} \tag{49}$$

Two independent variables are chosen for use in the optimization: amount to superheat (T_{sh}) and pressure ratio (P/P_c). The amount of superheat is the temperature in degrees and over outlet pressures. Since inlet temperature is constant, the amount of superheat vapor changes when saturation temperature and pressure change. These particular variables are chosen because they have the largest effects on expander performance and efficiency [37]. Table 4 lists numerous variables and their bounds relative to the optimization.

Table 4. Upper and lower limits for important variables in the optimization.

Variable		Lower Bound	Upper Bound
Independent Variables	Pr	1.5	10
	T_{sh}	5	45
Critical Variables (Which	T_4 (°C)	30	100
Require Physical Limits)	ω	0	4000

Here, T_4 is the condenser outlet temperature, which is set so that it is not possible to go below 30 °C since the environment temperature in which it operates is 25 °C. The rotational speed is set so that it cannot go below 0 or over 4000 rpm, which is a practical limit for this particular expander.

4. Results and Discussion

For the system optimization, two independent parameters are selected as objective functions. In this case, the function to be optimized is exergy efficiency and the two independent variables are pressure ratio (P_r) and degree of superheat (T_{sh}). The exergy efficiency function may not be related directly to pressure ratio and degree of superheat, but these two variables notably affect output power and the amount of required heat input. These two characteristics affect the exergy efficiency, since it is dependent both on electrical work output and heat input. Figures 3 and 4 show the values of T_{sh} and P_r optimized for each of the working fluids. All of the dry fluids (e.g., R227ea, R134a, n-pentane, and R123) according to the specified constraints require a higher superheated temperature, which lies near the limit specified for the system. This limitation is due to the restrictions in condenser temperature, which taken to be 30 °C.
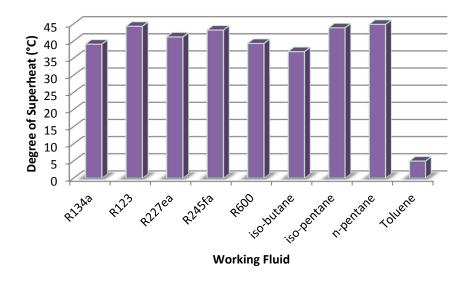
Figure 3. Optimized values of degree of superheat for considered working fluids.
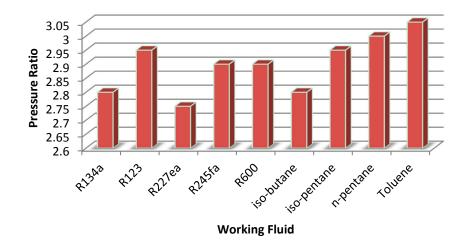

Figure 4. Optimized values of pressure ratio for considered working fluids.

N-pentane exhibits the highest degree of superheat (44.9 °C) and Toluene the lowest (5 °C). The pressure ratio varies from 2.75 for R227ea to 3.3 for water. Increasing isentropic efficiency produces more output power, which increases system exergy efficiency. Depending on the working fluid, a higher degree of superheat may increase isentropic efficiency. When superheat is increased, the pressure ratio increases slightly for most fluids. The system exergy efficiencies for various working fluids are shown in Figure 5, where values range from 15.4% for toluene to 21.9% for iso-butane. Systems using the working fluids iso-butane, R600 and R134a have the highest exergy efficiencies.
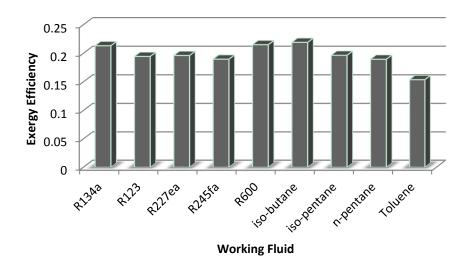
Figure 5. System exergy efficiency for various working fluids.

In Table 5, the value of exergy efficiency, energy efficiency, isentropic efficiency, electricity cost rate, power output, expander rotational speed, pressure difference and system input heat are presented for the optimal condition.

Table 5. Optimized thermodynamic parameter values for various working fluids.

Fluid	$\eta_{ex}\%$ Exergy Efficiency	$\eta_{th}\%$ Thermal Efficiency	$\eta_s\%$ Isentropic Efficiency	c_e (USD/kWh)	$\dot{W}_{elec}$ (kW)	Ω (RPM)	ΔP (kPa)	$\dot{Q}_{inb}$ (kW)
R134a	21	6.1	52	0.08	0.40	3917	1389.3	7.70
R123	19	5.5	52	0.49	0.06	655	222	1.30
R227ea	20	5.6	51	0.15	0.20	3053	920.7	4.30
R245fa	19	5.4	52	0.29	0.10	684.9	366	2.28
R600	22	6.1	51	0.14	0.23	1021	539	4.35
Iso-butane	22	6.2	52	0.10	0.30	1009	745.5	5.70
Iso-pentane	20	5.6	51	0.36	0.084	939	212.5	1.76
n-pentane	19	5.4	50	0.46	0.065	937	165.3	1.43
Toluene	15	4.4	50	1.43	0.021	836	58.3	0.56

Since exergy efficiency is a function of electrical work output and heat input, energy efficiency can be considered to be maximized when exergy efficiency is maximized, as they depend on the same variables. The lowest energy efficiency occurs for the working fluid toluene (4.4%) and the highest for iso-butane (6.2%). Systems using R600 and R134a exhibit relatively high energy efficiencies, both about 6.1%. The R600 and R134a fluids are appropriate for use in organic Rankine cycles as they provide the best efficiencies under the analyzed conditions.

The isentropic efficiency of the expander is important in determining the amount of useful work it produces. Lower isentropic efficiencies mean that there are significant losses internally. As the fluid is expanded, the potential work instead is lost in overcoming friction and leakage losses. The isentropic efficiency for most working fluids considered is at or near the maximum value at the given conditions.

The isentropic efficiency is considered to be at a maximum if the pressure after the isochoric pressurization section is the same as the condenser pressure. If the pressures are higher or lower, throttling or additional work input are needed. These additional processes introduce irreversibilities since they do not contribute to useful work. High pressure ratios introduce additional leakage since the leakage mass flow rate is a function of input and output pressures. The system expander using R134a has the highest isentropic efficiency (52%) while that using n-pentane has the lowest (50.3%). These values are relatively low and suggest that this expander has significant losses due to friction and leakage.

From the exergo-economic analysis, the unit cost of electricity is calculated with the optimized results. The results are useful in identifying which fluid has the lowest electrical output unit cost. From Table 5, toluene and R123 have unit electrical costs of 1.14 USD/kWh and 0.49 USD/kWh, respectively, which are the highest of all the working fluids considered. Systems using R134a, iso-butane and R600 exhibit the lowest unit costs of electricity, with values of 0.08, 0.10 and 0.14 USD/kWh, respectively. These costs reflect the lowest price that needs to be charged for the electricity and depend significantly on the amount of work output. The working fluids with the highest unit cost for electricity are seen to have the lowest electrical work outputs. Conversely, the working fluids with the highest electrical work outputs have the lowest electricity rates. For instance, systems using R134a, iso-butane and R600 generate 396.7, 301.7 and 226 W of electrical power, respectively, while those using toluene and R123 generate 20.8 and 61.3 W of electrical power, respectively.

The difference in pressure from inlet to outlet for the expander plays a large role in determining its work output. Since the torque produced by the expander is directly related to this pressure difference, it is useful to analyze this effect to help explain the work outputs of systems using each working fluid. The expander using R134a has the highest pressure difference (1389 kPa) and that using toluene the lowest (58.3 kPa). Other working fluids like R123 and n-pentane exhibit a low pressure difference, which corresponds to low electrical power outputs. The work output rate also corresponds to the heat input rate needed by the system. Systems using working fluids that lead to high work output rates such as R134a and iso-butane have high heat input rates. The system using R134a requires a heat input rate of almost 7.7 kW to produce 396.7 W of electrical power. The lowest heat input rate is needed for the system using toluene, which requires a heat input of 560 W to generate 20.8 W of electricity.

4.1. Exergy Analysis

Table 6 shows the exergy destruction breakdown for the system for each working fluid considered. The exergy destruction rate for the overall system using R134a is 1.3 kW. Most of the exergy destruction occurs is in the boiler (59.7%), and is due to the irreversible heat transfer processes in that component. The expander is responsible for almost 32% of the exergy destruction. These results suggest that there the improvement potentials are large for these components. This large share of exergy destruction in the expander is a consequence of the low expander isentropic efficiency of 52%. Large-scale systems typically have much higher expander isentropic efficiencies, approaching 80% to 90%. In order for the systems considered here to be competitive, the isentropic efficiency of its expander likely needs to improve. For the system using R227ea, the boiler is responsible for most of the system exergy destruction. Due to the larger amount of regeneration needed for this fluid (since it is a dry fluid), it exhibits relatively more exergy destruction in the regenerator. The condenser exergy destruction is

also low for this system, and this can be attributed to the low temperature differences between the environment and the working fluid at the input state (see Table 1). There are large improvement potentials for the boiler and the expander. The system using toluene has the lowest power production and has a large exergy destruction rate in the expander. The systems using iso-pentane and n-pentane have similar exergy destruction rates for the expander and the boiler. This is due to their similar chemical makeup of the working fluids. Note, however, that the exergy destroyed in the condenser is higher for the system using n pentane than the one using iso-pentane. Table 6 shows the exergy destruction breakdowns for the systems using various working fluids. These results can help guide the selection of working fluid.

Table 6. Working fluid exergy destruction percentage breakdown.

Working Fluid	Exergy Destruction (% of Total in System)				
	Boiler	**Expander**	**Condenser**	**Pump**	**Regenerator**
R134a	59.67	32.18	0.3	0.61	7.25
R123	65.44	25.76	0.35	0.08	8.37
R227ea	56.31	29.14	0.66	0.53	13.38
R245fa	64.53	25.99	0.09	0.13	9.25
R600	59.77	30.79	0.28	0.24	8.92
Iso-butane	57.91	32.07	0.25	0.39	9.37
Iso-pentane	63.16	26.46	0.25	0.09	10.04
n-pentane	64.16	25.61	0.58	0.06	9.59
Toluene	44.54	49.85	1.05	0.04	4.52

4.2. Exergo-Economic Analysis

The exergo-economic cost balance equations are used in the analysis to determine the unit cost rate of electricity for an optimized exergy efficiency. The equation for exergy efficiency depends on the electrical power output and the heat input rate. The maximized value of exergy efficiency does not necessarily represent the maximum power output for the system at a particular pressure ratio. Optimizing the cost of electricity for systems using R134a and iso-butane is done by requiring EES to minimize the function for c_e (electricity unit cost rate), which is found in the cost rate balance for the expander. The same two independent variables, pressure ratio and superheat, are used. The bounds for the analysis do not change. Five unit exergy costs for input heat are considered: 0.001, 0.002, 0.004, 0.006 and 0.008 USD/kWh. These costs are used for comparison purposes to assess the sensitivity of the system to such changes. The same assumptions are used as outlined in the exergo-economic analysis section. Figure 6 shows the minimized values for electricity rate for systems using R134a and iso-butane.
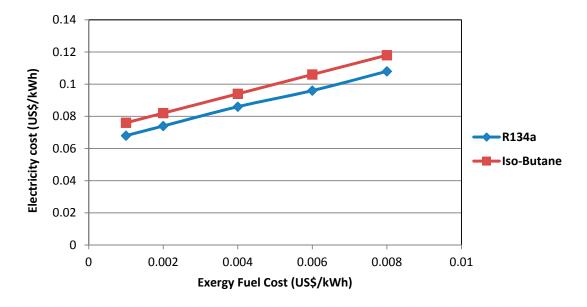
Figure 6. Optimized values of electricity rate for systems using R134a and iso-butane working fluids.

Thermal efficiency is dependent on two parameters including input heating energy and electricity output although the cost of electricity is dependent on the power output of the system so increase the cost of electricity is not necessarily reduced thermal efficiency. Figure 7 shows the relationship between cost of electricity and thermal efficiency for R134a in the superheat temperature between 10 and 45 °C and the pressure ratio is 2.8.
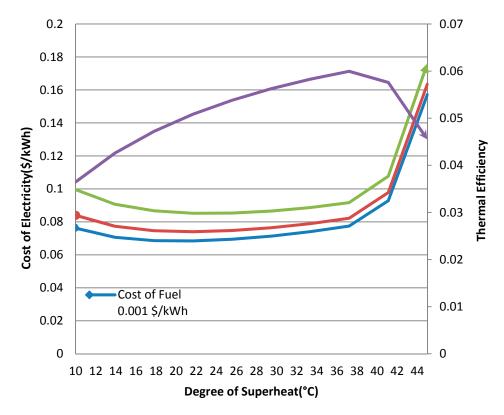

Figure 7. Electricity cost rate and thermal efficiency with varying superheat at optimal pressure ratio and three different fuel costs (R134a).

5. Conclusions

Energy, exergy and exergo-economic analyses and optimizations are performed on a scroll based organic Rankine cycle to improve performance within physical constraints. Various fluids are tested to identify the best performing fluid for the application considered. The working fluid toluene exhibits poor performance in this system due to the low pressure drop through the expander compared to systems using other fluids. R134a and iso-butane show promising results for use as working fluids in organic Rankine cycles, and permit high power outputs. The electrical power output is found to be important since it directly correlates with cost rate to produce it. The exergy efficiencies for systems using R134a and iso-butane are 21.3% and 21.9%, respectively, and most of the exergy losses occur in the boiler and expander for all working fluids. The system using R134a has the lowest cost rate for electricity at 0.07 USD/kWh (C_e = 0.001 USD/kWh) at the lowest fuel input cost and 0.1 USD/kWh at the highest fuel input cost (C_e = 0.008 USD/kWh). The present results are consistent with those reported in the literature by others [13]. The results in the present study show that systems using R134a and iso-butane have the highest energy and exergy efficiencies for heat source temperatures of 120 °C. These results are consistent with those given above for two other studies.

Author Contributions

All authors have read and approved the final manuscript.

Conflicts of Interest

The authors declare no conflict of interest.

Nomenclature

A_f	Amortization factor
BVR	Built in volume ratio of expander
c (USD/kWh)	Unit exergy cost
$\dot{C}$ (USD/h)	Exergy cost rate
e_x (kJ/kg)	Specific exergy
$\dot{E}x$ (kW)	Exergy rate
i (%)	Interest rate
ICC (USD)	Initial capital cost
k_p	Pressure torque coefficient
k_ω	Angular velocity torque coefficient
$\dot{m}$ (kg/s)	Total mass flow rate
$\dot{m}_{exp}$ (kg/s)	Expander mass flow rate
$\dot{m}_{leak}$ (kg/s)	Leakage mass flow rate
$\dot{m}_{pocket}$ (kg/s)	Mass of Pocket
N	Number of years
OM (USD)	Operating and maintenance cost
OM%	Percentage of operating and maintenance of initial capital cost

ORC	Organic Rankine cycle
Δp (kPa)	Difference in pressure
P (kPa)	Pressure
P_C (kPa)	Critical pressure Specific heat
q(kj/kg)	Specific heat input or output
$\dot{Q}$ (kW)	Heat rate
T (°C)	Temperature
T (s)	Time
TCC (USD)	Total capital cost
v (m^3/kg)	Specific volume
$\dot{W}$ (kW)	Rate of work (or power)
$\dot{Z}$ (USD/h)	Operating rate for component
Greek Letters	
Z	Expander leakage coefficient
H	Efficiency
Π	Isochoric pressure building coefficient
τ (N. m)	Torque
ω (rad/s)	Angular velocity

References

1. Davidson, T.A. Design and Analysis of a 1 kW Rankine Power Cycle, Employing a Multi-Vane Expander, for Use with a Low Temperature Solar Collector. Master's Thesis, Massachusetts Institute of Technology, Cambridge, MA, USA, 1977.

2. Probert, S.D.; Hussein, M.; O'Callaghan, P.W.; Bala, E. Design optimization of a solar-energy harnessing system for stimulating irrigation pump. *Appl. Energy* **1983**, *15*, 299–321.

3. Monahan, J. Development of a 1-kW, Organic Rankine Cycle Power Plant for remote applications. In Proceedings of the Intersociety Energy Conversion Engineering Conference, New York, NY, USA, 12–17 September 1976.

4. Badr, O.; O'Callaghan, P.W.; Probert, S.D. Rankine-cycle systems for harnessing power from low-grade energy sources. *Appl. Energy* **1990**, *36*, 263–292.

5. Nouman, J. Comparative Studies and Analyses of Working Fluids for Organic Rankine Cycles—ORC. Master's Thesis, KTH School of Industrial Engineering and Management, Sweden, 2012.

6. Andersen, W.C.; Bruno, T.J. Rapid screening of fluids for chemical stability in organic Rankine cycle applications. *Ind. Eng. Chem. Res.* **2005**, *44*, 5560–5566.

7. Hung, T.C.; Shai, T.Y.; Wang, S.K. A review of organic Rankine cycles (ORCs) for the recovery of low-grade waste heat. *Energy* **1997**, *22*, 661–667.

8. Angelino, G.; Colonna, D.I. Multi component working fluids for organic Rankine cycles (ORCs). *Energy* **1998**, *23*, 449–463.

9. Yamamoto, T.; Furuhata, T.; Arai, N.; Mori, K. Design and testing of the organic Rankine cycle. *Energy* **2001**, *26*, 239–251.

10. Nguyen, V.M.; Doherty, P.S.; Riffat, S.B. Development of a prototype low-temperature Rankine cycle electricity generation system. *Appl. Therm. Eng.* **2001**, *21*, 169–181.

11. Wei, D.; Lu, X.; Lu, Z.; Gu, J. Performance analysis and optimization of organic Rankine cycle (ORC) for waste heat recovery. *Energy Convers. Manag.* **2007**, *48*, 1113–1119.

12. Saleh, B.; Koglbauer, G.; Wendland, M.; Fischer, J. Working fluids for low temperature organic Rankine cycles. *Energy* **2007**, *32*, 1210–1221.

13. Mago, P.J.; Chamra, L.M. Exergy analysis of a combined engine-organic Rankine cycle configuration. *Proc. Inst. Mech. Eng. A* **2008**, *222*, 761–770.

14. Mago, P.J.; Chamra, L.M.; Srinivasan, K.; Somayaji, C. An examination of regenerative organic Rankine cycles using dry fluids. *Appl. Therm. Eng.* **2008**, *28*, 998–1007.

15. Chacartegui, R.; Sánchez, D.; Munoz, J.; Sánchez, T. Alternative ORC bottoming cycles for combined cycle power plants. *Appl. Energy* **2009**, *86*, 2162–2170.

16. Dai, Y.; Wang, J.; Gao, L. Parametric optimization and comparative study of organic Rankine cycle (ORC) for low grade waste heat recovery. *Energy Convers. Manag.* **2009**, *50*, 576–582.

17. Quoilin, S.; Declaye, S.; Tchanche, B.; Lemort, V. Thermo-economic optimization of waste heat recovery Organic Rankine Cycles. *Appl. Therm. Eng.* **2011**, *31*, 2885–2893.

18. Wang, E.H.; Zhang, H.G.; Fan, B.Y.; Ouyang, M.G.; Zhao, H.; Mu, H.Q. Study of working fluid selection of organic Rankine cycle (ORC) for engine waste heat recover. *Energy* 2011, *12*, 3406–3418.

19. Qiu, G. Selection of working fluids for micro-CHP systems with ORC. *Renew. Energy* 2012, *45*, 565–570.

20. Kang, S.H. Design and experimental study of ORC (organic Rankine cycle) and radial turbine using R245fa working fluid. *Energy* 2012, *41*, 514–524.

21. Wang, M.; Wang, J.; Zhao, Y.; Dai, Y. Thermodynamic analysis and optimization of a solar-driven regenerative organic Rankine cycle (ORC) based on flat-plate solar collectors. *Appl. Therm. Eng.* **2013**, *50*, 816–825.

22. Quoilin, S.; Declaye, S.; Tchanche, B.; Lemort, V. Techno-economic survey of Organic Rankine Cycle (ORC) systems. *Renew. Sustain. Energy Rev.* 2013, *22*, 168–186.

23. Clemente, S.; Micheli, D.; Reini, M.; Taccani, R. Bottoming organic Rankine cycle for a small scale gas turbine: A comparison of different solutions. *Appl. Energy* 2013, *106*, 355–364.

24. Branchini, L.; de Pascale, A.; Peretto, A. Systematic comparison of ORC configurations by means of comprehensive performance indexes. *Appl. Therm. Eng.* 2013, *61*, 129–140.

25. Lecompte, S.; Huisseune, H.; vandenBroek, M.; de Schampheleire, S.; de Paepe, M. Part load based thermo-economic optimization of the Organic Rankine Cycle (ORC) applied to a combined heat and power (CHP) system. *Appl. Energy* **2013**, *111*, 871–881.

26. Zabek, D.; Penton, J.; Reay, D. Optimization of waste heat utilization in oil field development employing a transcritical Organic Rankine Cycle (ORC) for electricity generation. *Appl. Therm. Eng.* 2013, *59*, 363–369.

27. Bracco, R.; Clemente, S.; Micheli, D.; Reini, M. Experimental tests and modelization of a domestic-scale ORC (Organic Rankine Cycle). *Energy* 2013, *58*, 107–116.

28. Wang, D.; Ling, X.; Peng, H.; Liu, L.; Tao, L. Efficiency and optimal performance evaluation of organic Rankine cycle for low grade waste heat power generation. *Energy* 2013, *50*, 343–352.

29. Yu, G.; Shu, G.; Tian, H.; Wei, H. Simulation and thermodynamic analysis of a bottoming Organic Rankine Cycle (ORC) of diesel engine (DE). *Energy* 2013, *51*, 281–290.

30. Li, M.; Wang, J.; He, W.; Gao, L.; Wang, B.; Ma, S.; Dai, Y. Construction and preliminary test of a low-temperature regenerative Organic Rankine Cycle (ORC) using R123. *Renew. Energy* 2013, *57*, 216–240.

31. Maraver, D.; Royo, J.; Lemort, V.; Quoilin, S. Systematic optimization of subcritical and transcritical organic Rankine cycles (ORCs) constrained by technical parameters in multiple applications. *Appl. Energy* 2014, *117*, 11–29.

32. Meinel, D.; Wieland, C.; Spliethoff, H. Effect and comparison of different working fluids on a two-stage organic rankine cycle (ORC) concept. *Appl. Therm. Eng.* 2014, *63*, 246–253.

33. Mago, P.J.; Chamra, L.M.; Somayaji, C. Analysis and optimization of organic Rankin cycles. *IMechE J. Power Energy* 2007, *221*, 255–263.

34. Xianbiao, B.; Wang, L.B.; Li, H.S. Performance analysis and working fluid selection for geothermal energy-powered organic Rankine-vapor compression air conditioning. *Geotherm. Energy* 2013, doi:10.1186/2195-9706-1-2.

35. Oralli, E.; Tarique, M.D.A.; Zamfirescu, C.; Dincer, I. A study on scroll compressor conversion into expander for Rankine cycles. *Int. J. Low Carbon Technol.* **2011**, *6*, 200–206.

36. Tarique, M.D.A. Experimental Investigation of Scroll Based Organic Rankine Systems. Master's Thesis, University of Ontario Institute of Technology, Oshawa, ON, Canada, 2011.

37. Nafey, A.S.; Sharaf, M.A.; Garcia-Rodriguez, L. Thermo-economic analysis of a combined solar organic Rankine Cycle-reverse osmosis desalination process with different energy recovery configurations. *Desalination* **2010**, *261*, 138–147.